Role of Platinum in Photoelectrochemical Studies Related to Solar Energy Harvesting

http://dx.doi.org/10.1595/147106712X654178 http://www.platinummetalsreview.com/

By Kasem K. Kasem

Science, Mathematics, and Informatics Department, Indiana University Kokomo, Kokomo, IN 46904-9003, USA

Email: kkasem@iuk.edu

The electrochemical behaviour of platinum as a regenerator electrode during the photolysis of buffered aqueous solutions of ferrocyanide ($[Fe(CN)_6]^{4-}$) as a source of hydrated electrons for hydrogen production was investigated. Optimum conditions for the heterogeneous reduction of ferricyanide ($[Fe(CN)_6]^{3-}$) in aqueous suspensions of semiconductor nanoparticles were determined, and hydrogen generation was explored in both homogeneous and heterogeneous aqueous systems. Experiments took place in a three-electrode cell. The results indicated that the Pt gauze electrode gave adequate and reproducible photoelectrochemical performance during the photolysis of aqueous solutions of $[Fe(CN)_6]^{4-}$ in 0.2 M pH 6 phosphate buffer. The results provide evidence for the important role of Pt in photolysis studies that aim towards harvesting solar energy.

Introduction

The stability domain of Pt almost completely overlaps the stability domain of water as a result of the very noble nature of Pt. In comparison with the other elements in its group, Pt possesses the greatest zone of immunity to corrosion over the entire pH scale. **Figure 1** is the Pourbaix diagram (1) for Pt and gold and shows their respective zones of stability in water at room temperature. According to **Figure 1**, Au has a wider potential window of immunity against corrosion than does Pt. However, the data show the oxidation of water to oxygen at different pHs below the immunity line of Au and this fact limits the use of Au in tracing the photolysis of water in aqueous systems containing redox couples with more positive potentials than those studied using Pt.

Historically, the use of Pt electrodes in electrochemical cells has been well known. Traditionally, Pt electrodes have been used for H_2 production by the electrolysis of water. However, the use of Pt in photoelectrochemical studies has only recently been reported (2–8). These include investigations of the photoelectrochemical behaviour of platinum/titanium dioxide (Pt/TiO_2)

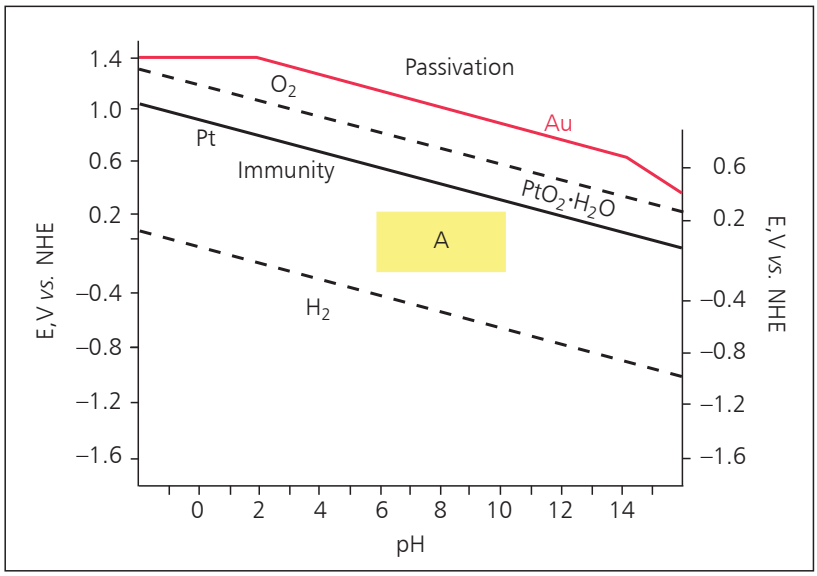

Fig. 1. Pourbaix diagram for platinum and gold (1)

nanocomposite thin film electrodes (2, 3, 5, 6), as well as reports on the role of Pt in dye-sensitised solar cells (4), in the formation of metal hydrides (7) and in the photocatalytic degradation of 2,4,6-trinitrotoluene (TNT) (8). Other studies have used modified Pt electrodes with chlorophyll liquid crystals for photosynthesis (9), with mercury(II) sulfide (10) in photodegradation applications, and to enhance the activity of H_2 production and the dechlorination of tetrachloromethane (CCl_4) (11).

The $[Fe(CN)_6]^{4-}/[Fe(CN)_6]^{3-}$ aqueous system is used to capture energy from solar radiation by the formation of hydrated electrons. Hydrated electrons can play an important role in the photodissociation of water through Reactions (i)–(iii):

$$[Fe(CN)_6]^{4-} + h\nu \rightarrow [Fe(CN)_6]^{3-} + e^-_{aq} \quad \text{(i)}$$

$$e^-_{aq} + e^-_{aq} \rightarrow H_2 + 2OH^- \quad \text{(ii)}$$

$$2[Fe(CN)_6]^{4-} + 2h\nu \rightarrow 2[Fe(CN)_6]^{3-} + H_2 + 2OH^- \quad \text{(iii)}$$

$[Fe(CN)_6]^{4-}$ undergoes photooxidation to $[Fe(CN)_6]^{3-}$ as shown in Reaction (i) (12). The molecular orbital structure of $[Fe(CN)_6]^{4-}$ allows electronic transitions under the photo-excitation condition. This will produce hydrated electrons that react according to Reaction (ii), with a rate constant $k \approx 1 \times 10^{10}$ M^{-1} sec^{-1} (13). The overall reaction is shown in Reaction (iii).

The disadvantage of a homogeneous process for H_2 production is its irreversibility, as indicated by Reaction (i). Because $[Fe(CN)_6]^{4-}$ is the photoactive agent that captures the visible light, it is important that $[Fe(CN)_6]^{4-}$ be regenerated in order to create the conditions for a reversible process. The perfect conditions could be reached if the rate of reduction of $[Fe(CN)_6]^{3-}$ were closer to the rate of formation of hydrated electrons from $[Fe(CN)_6]^{4-}$.

One of the ways to achieve this goal is through the use of a semiconductor system which acts as an electron donor and reduces $[Fe(CN)_6]^{3-}$ back to $[Fe(CN)_6]^{4-}$, as illustrated in Reaction (iv):

$$2[Fe(CN)_6]^{3-} + (e/h)\ (\text{from SC}) \rightarrow 2[Fe(CN)_6]^{4-} \quad \text{(iv)}$$

in which e/h is the electron/hole pair and SC is the semiconductor.

Previous studies have used semiconductor particles as a major means of photon capture and conversion through heterogeneous charge transfer processes at the particle/electrolyte interface (14–16). Some of the problems associated with this method are electron/hole recombination and possible side reactions. An alternative approach is to use electrochemical reduction in which the potential of a Pt electrode is fixed at the reduction potential of aqueous $[Fe(CN)_6]^{3-}$ using an external electromotive force (EMF) source. Although the kinetics of the reduction of $[Fe(CN)_6]^{3-}$ on a Pt electrode are fast and effective, the disadvantage of the electroreduction method is the need to use an external EMF source. However, this disadvantage can be overcome if the external

EMF source is operating using photovoltaic solar cells (**Figure 2**).

In this paper, the electrochemical behaviour of Pt as a regenerator electrode (cathode) to ensure full reversibility of Reaction (i) is investigated in aqueous pH 6 phosphate buffer containing 0.02 M $[Fe(CN)_6]^{4-}$ in the absence and presence of colloidal cadmium sulfide (CdS) or titanium dioxide/vanadium(V) oxide (TiO_2/V_2O_5) (1:1) nanoparticles.The current generated by the Pt regenerator electrode under illumination will be used to examine the usefulness of Pt as an effective working electrode in photoelectrochemical studies.

Experimental

All the reagents were of analytical grade. All of the solutions were prepared using deionised water, unless otherwise stated.

All electrochemical experiments were carried out using a conventional three-electrode cell with Pt wire as a counter electrode, silver/silver chloride (Ag/AgCl) as a reference electrode, and Pt gauze as working electrode. A BAS 100W Electrochemical Analyzer (Bioanalytical Systems, Inc, USA) was used to perform the electrochemical studies. Steady state reflectance spectra were recorded using a Shimadzu UV-2101 PC spectrophotometer (Shimadzu Corp, USA). An Olympus BX-FLA reflected light fluorescence microscope (Olympus Corp, Japan) working with polarised light at a wavelength range between 330 nm and 550 nm was used to ensure that the diameter of the colloidal nanoparticles did not exceed 200 nm. For this study H_2 gas was detected using a HY-ALERTA™ 500 Handheld Hydrogen Leak Detector (H2scan,USA). Quantitative determination of H_2 and confirmation of the stoichiometry of Reaction (iii) has been previously accomplished (12).

The electrolysis cell was a 120 ml one-compartment Pyrex cell with a quartz window facing the irradiation source. A 10 cm^2 Pt gauze cylinder was used as the regenerator electrode. Aqueous suspensions were stirred with a magnetic stirrer during the measurements. The cell design is displayed in **Figure 2**. An Ag/AgCl/Cl^- reference electrode was also fitted into this compartment. A 10 cm^2 Pt counter electrode was housed in a glass cylinder sealed at one end with a fine porosity glass frit.The pH was adjusted by addition of either 1 M sodium hydroxide (NaOH) or 1 M nitric acid (HNO_3).The external EMF used in this study was supplied by a traditional potentiostat in place of the photovoltaic generator and light-powered potentiostat indicated in **Figure 2**.

Irradiations were performed with a solar simulator 300 W xenon lamp (Newport Corp, USA) with an infrared (IR) filter. Light was focused on the cell

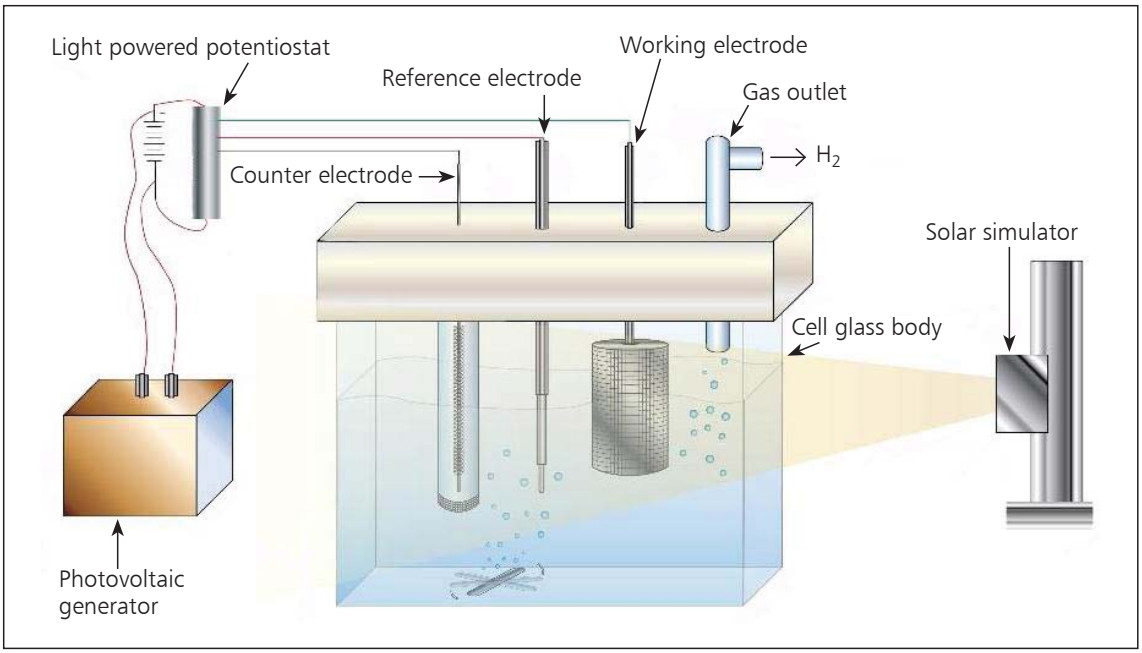

Fig. 2. Diagram of a photolysis cell

window using a metal cylinder 5 cm in diameter, and 15 cm long. The cell position was adjusted to allow full illumination of the 100 ml suspension. Photolysis of $[Fe(CN)_6]^{4-}$ generated hydrated electrons and $[Fe(CN)_6]^{3-}$. The potential of the working electrode was fixed at 0.0 V *vs.* Ag/AgCl, which was 100 mV more negative than the reduction potential of $[Fe(CN)_6]^{3-}$ to guarantee full reduction of ferricyanide. The current due to the reduction of $[Fe(CN)_6]^{3-}$ collected by the working electrode during the photolysis process is a measure of photocurrent. Photocurrent-time curves were obtained using a BAS 100W Electrochemical Analyzer.

Results and Discussion

Effect of Pretreatment of Platinum Electrode

The Pt electrode was cleaned before use with 1:1 HNO_3, rinsed with deionised water, dried, and heated at 1100ºC for 3 minutes. The activation of the Pt electrode was tested by cyclic voltammetry (CV) in 0.2 M sulfuric acid (H_2SO_4) and the H_2 reduction peak was identified in the generated CV trace. Pt electrodes treated this way gave the greatest reduction current during the photolysis of 0.2 M $[Fe(CN)_6]^{4-}$ under the selected conditions.

Aqueous System for Hydrogen Production Using Photolysis

Two factors were used to overcome the irreversibility of Reaction (i) and to regenerate $[Fe(CN)_6]^{4-}$:

(a) use of a suspension of semiconductor nanoparticles; and

(b) fixing the potential of the Pt regenerating electrode at 0.0 V *vs.* Ag/AgCl/Cl^-.

Both the Pt electrode and the semiconductor nanoparticles serve as electron donors to reduce $[Fe(CN)_6]^{3-}$ back to $[Fe(CN)_6]^{4-}$.

Reaction (i) was assumed to be fully reversible at the Pt electrode surface at pH 6 since photodecomposition of $[Fe(CN)_6]^{3-}$ at pH 6 is highly unlikely (17, 18). Photodecomposition of $[Fe(CN)_6]^{3-}$ may take place at pH > 10 (17) under several hours of illumination with ultraviolet (UV) light (18). The stability of $[Fe(CN)_6]^{3-}$ was confirmed by tracing the changes in $[Fe(CN)_6]^{3-}$ concentration using differential pulse voltammetry (DPV) during 2 hours of illumination.

Electrochemical Behaviour of Platinum Electrode in Phosphate Buffer at Different pHs

Because one of the products of photochemical Reaction (iii) is OH^-, this reaction is pH dependent. This also suggests that pH < 7 would be suitable to shift the equilibrium of the reaction to favour H_2 production. However, an important factor should be considered in choosing a suitable electrode for reduction of $[Fe(CN)_6]^{3-}$. It is important that the electrode must be in a pure state and that no oxides will be formed on the surface that could affect the kinetics of the reduction process. The Pourbaix diagram (1) for platinum/water at 25ºC, displayed in **Figure 1**, indicates that Pt is not subject to corrosion and is in its pure form within the potential range of –0.1 to 0.3 V *vs.* standard hydrogen electrode (SHE) at pH 6. This range is narrowed as pH increases (**Figure 1**, shaded zone A). Furthermore, it was found that at pH less than 6, $K_4[Fe(CN)_6]$ will form a green compound known as Berlin green (BG) or ferric ferricyanide $Fe[Fe(CN)_6]$. This product formation limits the pH range for the study to pH ≥ 6.

Reduction currents were recorded during the photolysis of aqueous $K_4[Fe(CN)_6]$ in phosphate buffer at different pH values, using a Pt electrode. The results are displayed in **Figure 3**. It can be noticed that a drop in the reduction current occurs at pH values greater than 6. This can be attributed to the fact that $K_4[Fe(CN)_6]$, under photolysis conditions, is pH sensitive. For these reasons, photolysis of aqueous $K_4[Fe(CN)_6]$ in the presence of CdS or TiO_2/V_2O_5 nanoparticles was conducted at pH 6.

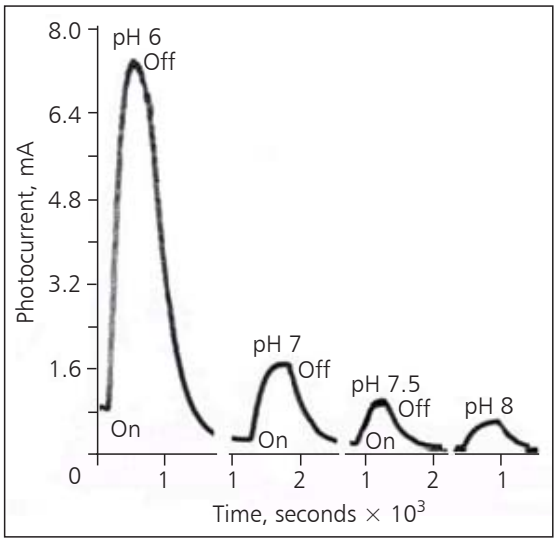

Fig. 3. Effect of pH on the reduction current recorded by the Pt working electrode

Comparison of Electrochemical Behaviour of Platinum Electrode in Heterogeneous and Homogeneous Systems

Nanoparticles in the suspension system used in these studies cannot be subject to the traditional classification of semiconductors as n- or p-types. This is because, in isolated nanoparticle suspensions, neither the hole nor the electron can be collected and transferred through conductors to outside donors or acceptors. Instead, they act as a 'nano cell'. Charge separation can be achieved either by neutralising the positive holes (h) using hole scavengers such as multi-charged anions, or by capturing one or more electrons using appropriate Lewis acids. The kinetics of each process will determine which process predominates.

The reduction current was recorded for the Pt electrode during the photolysis of aqueous $K_4[Fe(CN)_6]$ in the presence of CdS or TiO_2/V_2O_5 nanoparticles at pH 6. The results are displayed in **Figure 4**. **Figures 4** and **5** show that:

- Photolysis of a homogeneous solution of $[Fe(CN)_6]^{4-}$ reaches a peak current greater than that recorded in the heterogeneous system (peak of section A and peak of section B in **Figure 4**).
- Photolysis of a homogeneous solution generates a very short plateau, while the photolysis of a heterogeneous suspension containing $[Fe(CN)_6]^{4-}$ (in the presence of semiconductor nanoparticles) produces a longer plateau (**Figure 5**).

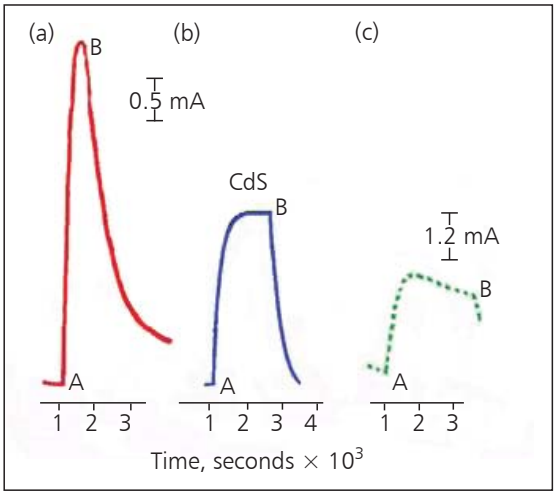

Fig. 4. Photoelectrochemical response of the platinum working electrode during the photolysis of 20 mM $K_4[Fe(CN)_6]$ in 0.2 M phosphate buffer at pH 6: (a) homogeneous solution only; (b) in presence of CdS colloidal nanoparticles; (c) in presence of TiO_2/V_2O_5 (1:1) colloidal nanoparticles. Points A and B refer to illumination and dark, respectively

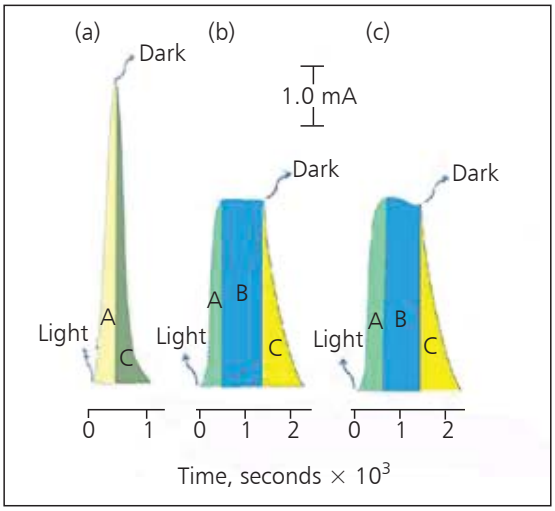

Fig. 5. Diagram illustrating the portions of the current-time plots for photolysis of 20 mM $K_4[Fe(CN)_6]$ in 0.2 M phosphate buffer at pH 6: (a) homogeneous system; (b) heterogeneous system with steady adsorption/desorption equilibrium; (c) heterogeneous system without steady adsorption/desorption equilibrium. The areas labelled A represent direct reduction of $[Fe(CN)_6]^{3-}$ generated without adsorption; the areas labelled B represent direct reduction of form due to adsorption; and the areas labelled C represent dark current

The smaller peak height in the heterogeneous system than in the homogeneous system can be explained as follows. When oxide nanoparticles are added to $[Fe(CN)_6]^{4-}$ solutions, Reaction (v) takes place:

$$M^{z+}\text{ (solubility equilibrium)} + [Fe(CN)_6]^{4-} \rightarrow M\{[Fe(CN)_6]^{4-z}\}_{(s)} \quad (v)$$

where M is Cd, Ti or V and z is the charge on M.

$M\{[Fe(CN)_6]^{4-z}\}_{(s)}$ will stabilise the surface against photodegradation (19, 20). Calculations based on particle size (100 nm radius), CdS and TiO_2 lattice parameters, and the stoichiometry of Reaction (v) indicate that the amount of $[Fe(CN)_6]^{4-}$ consumed in Reaction (v) is less that 0.06% of its original concentration of 20.0 mM l^{-1}. Following this, $[Fe(CN)_6]^{4-/3-}$ (the product of Reaction (i)) is adsorbed on the surface of the nanoparticles (21–23). Adsorption decreases the amount of $[Fe(CN)_6]^{4-}$ oxidised in Reaction (i), while adsorption of $[Fe(CN)_6]^{3-}$ reduces the amount of free $[Fe(CN)_6]^{3-}$ that can reach the Pt regenerator electrode. In both cases the recorded reduction current will be less than that reported in the homogeneous system. However, under illumination all of the $[Fe(CN)_6]^{4-}$

will be oxidised to $[Fe(CN)_6]^{3-}$ and the surface of the nanoparticles will be covered only with $[Fe(CN)_6]^{3-}$. This amount of $[Fe(CN)_6]^{3-}$ will be identified from now on as $\{[Fe(CN)_6]^{3-}\}_{ads}$. This adsorbed ferricyanide will be photochemically reduced at the nanoparticle surface.

The very small amount of $[Fe(CN)_6]^{4-}$ consumed in making the insoluble layer (<0.05%) suggests that adsorption phenomena are the main factors that explain why the reduction current recorded by the Pt regenerator electrode in the presence of nanoparticles is lower than that observed in the homogeneous solution.

The relatively high concentration of the dihydrogen phosphate anion ($H_2PO_4^-$) (0.2 M) in comparison with that of $[Fe(CN)_6]^{4-}$ (0.02 M) causes $H_2PO_4^-$ to be the major adsorbed species on the surface of the nanoparticles. The following mechanism is suggested for the photochemical reduction that leads to the reversibility of Reaction (i):

$$[Fe(CN)_6]^{4-} + h\nu \rightarrow [Fe(CN)_6]^{3-} + e^-_{aq} \quad \text{(i)}$$

First the $[Fe(CN)_6]^{3-}$ is adsorbed onto the semiconductor nanoparticles surface, Reaction (vi):

$$[Fe(CN)_6]^{3-} + \text{SC nanoparticles} \rightarrow \{[Fe(CN)_6]^{3-}\}_{ads} \quad \text{(vi)}$$

$H_2PO_4^-$ then acts as a hole scavenger and undergoes photooxidation to $H_2PO_4^*$ (24), as in Reaction (vii):

$$\text{SC (e/h)} + H_2PO_4^- \rightarrow H_2PO_4^* + \text{e (conduction band)} \quad \text{(vii)}$$

where e are electrons in the conduction band and h are holes in the valence band (**Figure 6**). Reaction (vii) is based on the fact that the calculated hole barrier heights (25) for the semiconductors used in this study range between 0.25 and 0.45 eV and are much smaller than the electron barrier heights. This suggests that hole transfer preferentially oxidises $H_2PO_4^-$, most likely due to its higher concentration compared to the $[Fe(CN)_6]^{4-}$ anion.

$\{[Fe(CN)_6]^{3-}\}_{ads}$ is then reduced to $\{[Fe(CN)_6]^{4-}\}_{ads}$ according to Reaction (viii):

$$\{[Fe(CN)_6]^{3-}\}_{ads} + \text{e (conduction band)} \rightarrow \{[Fe(CN)_6]^{4-}\}_{ads} \quad \text{(viii)}$$

$\{[Fe(CN)_6]^{4-}\}_{ads}$ is desorbed, Reaction (ix):

$$\{[Fe(CN)_6]^{4-}\}_{ads} \rightarrow \{[Fe(CN)_6]^{4-}\}_{desorb} \quad \text{(ix)}$$

The free $\{[Fe(CN)_6]^{4-}\}_{desorb}$ can then return to Reaction (i) to be photooxidised in homogeneous solution.

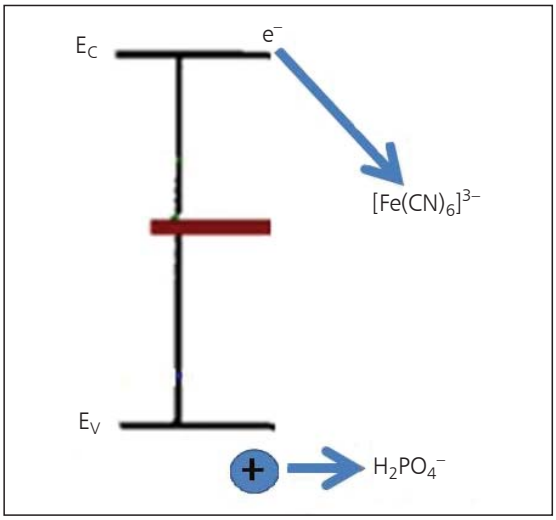

Fig. 6. Energy map for conduction (E_C) and valence (E_V) bands relative to the $[Fe(CN)6]^{3-}$ energy band

The portion of $[Fe(CN)_6]^{3-}$ generated by Reaction (i) and not adsorbed in Reaction (vi) and that reaches the Pt electrode to be reduced back is represented by the areas labelled A in **Figure 5**. The difference between area A in **Figure 5(a)** and the equivalent areas in **Figures 5(b)** and **5(c)** represents the amount of adsorbed $[Fe(CN)_6]^{3-}$ on the semiconductor nanoparticle surfaces. It can be concluded that the areas labelled A in **Figures 4** and **5** directly reflect the behaviour of the Pt generator electrode in the absence of semiconductor interference.

Electrochemical Behaviour of Platinum Electrode in the Presence of Semiconductor Nanoparticles

The plateaus in **Figures 4(b)** and **4(c)** and the areas labelled B in **Figures 5(b)** and **5(c)** represent the outcome of the above mechanism, and reflect the behaviour of the Pt regenerator electrode in the presence of semiconductor nanoparticles. These features also explain how the semiconductor nanoparticles made the reversibility of Reaction (i) possible. It is worth noting that the plateau current is either constant (as in **Figure 4(b)**) or slightly decreases with time (as in **Figure 4(c)**). This can be explained using **Figure 5**. Less adsorption will generate a lower drop in the peak reduction current reported for the Pt electrode (**Figure 5(a)**). The steady, constant reduction current at the plateau (**Figure 5(b)**) reflects an efficient reversible adsorption/desorption process (19, 23) at the semiconductor nanoparticle surfaces.

The slight decrease in the plateau shown in **Figure 4(c)** reflects less $[Fe(CN)_6]^{3-}$ reaching the Pt regenerator electrode. This can be attributed to the formation of Prussian blue-type insoluble compounds $Ti_x[Fe(CN)_6]_y$ and possibly $V_x[Fe(CN)_6]_y$ (20). These compounds will change the surface conditions and enhance the adsorption of $[Fe(CN)_6]^{3-}$ thereby decreasing the amount that reaches the Pt electrode. Withholding more $[Fe(CN)_6]^{3-}$ also indicates lack of equilibrium at the TiO_2/V_2O_5 semiconductor nanoparticle surfaces. The steady constant slope plateau in **Figure 4(b)** reflects the establishment of equilibrium at the CdS/Cd$[Fe(CN)_6]$ surface. The areas labelled B in **Figure 5** not only illustrate the extent of photon capture by the semiconductor nanoparticles during illumination, but also the efficiency of the semiconductor nanoparticles in cycling Reaction (i).

Dark Current

The behaviour of the Pt regenerator electrode in the absence of light can be explained by investigation of the areas labelled C in **Figure 5**, which represent electrochemical reduction current in the absence of light (dark current). In both the homogeneous and the heterogeneous systems studied in this work, the electrochemical reduction currents were expected to drop to zero in the dark. However this drop was not observed, as **Figure 4** illustrates. The reported electrochemical reduction current in the dark for the homogeneous phase of the system can be attributed to the radial diffusion of $[Fe(CN)_6]^{3-}$ in the cylindrical zone of the Pt gauze electrode (**Figure 2**). The shape of the working electrode disrupts the continuity of the stirring effects. This makes the diffusion within the cylindrical shape an important factor for the reduction current.

Conclusion

The electrochemical reduction current recorded for the Pt regenerator electrode during the photolysis of aqueous solutions of ferrocyanide in suspensions of semiconductor nanoparticles of CdS or TiO_2/V_2O_5 clearly indicates the usefulness of Pt as a regenerator electrode in water photolysis. When a reaction that can take place in a photoelectrochemical process has a redox potential within the potential range under which Pt is in its pure state, reliable results can be produced. Platinum is also expected to give better results over a wider range of conditions than gold, on the basis of its Pourbaix diagram.

References

1 M. Pourbaix, "Atlas of Electrochemical Equilibria in Aqueous Solutions", Pergamon Press, Oxford, UK, 1966, p. 361

2 T. Sasaki, W. T. Nichols, J.-W. Yoon and N. Koshizaki, *MRS Proc.*, 2004, **846**, DD8.10

3 K. Uosaki, R. Yoneda and H. Kita, *J. Phys. Chem.*, 1985, **89**, (19), 4042

4 C.-M. Chen, C.-H. Chen and T.-C. Wei, *Electrochim. Acta*, 2010, **55**, (5), 1687

5 C. He, M. A. Asi, Y. Xiong, D. Shu and X. Li, *Int. J. Photoenergy*, 2009, 634369

6 V. Subramanian, E. Wolf and P. V. Kamat, *J. Phys. Chem. B*, 2001, **105**, (46), 11439

7 S. Ohkubo, Y. Ashida, T. Utsumi, K. Hongo and G. Nogami, *J. Electrochem. Soc.*, 1996, **143**, (10), 3273

8 D. C. Schmelling, K. A. Gray and P. V. Kamat, *Environ. Sci. Technol.*, 1996, **30**, (8), 2547

9 M. Aizawa, J. Yoshitake and S. Suzuki, *Mol. Cryst. Liq. Cryst.*, 1981, **70**, (1–4), 1407

10 R. S. Davidson and C. J. Willsher, *Faraday Discuss. Chem. Soc.*, 1980, **70**, 177

11 W. Kim, T. Tachikawa, T. Majima and W. Choi, *J. Phys. Chem. C*, 2009, **113**, (24), 10603

12 K. Tennakone, S. Punchihewa and S. Abeysinghe, *J. Photochem. Photobiol. A: Chem.*, 1990, **51**, (2), 163

13 S. Gordon, E. J. Hart, M. S. Matheson, J. Rabani and J. K. Thomas, *J. Am. Chem. Soc.*, 1963, **85**, (10), 1375

14 R. Plass, S. Pelet, J. Krueger, M. Grätzel and U. Bach, *J. Phys. Chem. B*, 2002, **106**, (31), 7578

15 T. Mayer, R. Hunger, A. Klein and W. Jaegermann, *Phys. Status Solidi B*, 2008, **245**, (9), 1838

16 S. A. Haque, T. Park, A. B. Holmes and J. R. Durrant, *ChemPhysChem*, 2003, **4**, (1), 89

17 C. A. P. Arellano and S. S. Martínez, *Solar Energy Mater. Solar Cells*, 2010, **94**, (2), 327

18 X. Z. Yu, X. Y. Peng and G. L. Wang, *Int. J. Environ. Sci. Technol.*, 2011, **8**, (4), 853

19 H.-D. Rubin, D. J. Arent, B. D. Humphrey and A. B. Bocarsly, *J. Electrochem. Soc.*, 1987, **134**, (1), 93

20 K. Tennakone, *J. Phys. C: Solid State Phys.*, 1983, **16**, (34), L1193

21 J. Desilvestro, S. Pons, E. Vrachnou and M. Grätzel, *J. Electroanal. Chem. Interfacial Electrochem.*, 1988, **246**, (2), 411

22 W. P. Cheng, C. Huang and Y. C. Chien, *J. Colloid Interface Sci.*, 2000, **224**, (2), 291

23 C. M. Pharr and P. R. Griffiths, *Anal. Chem.*, 1997, **69**, (22), 4673

24 M. Abdullah, G. K. C. Low and R. W. Matthews, *J. Phys. Chem.*, 1990, **94**, (17), 6820

25 T. Lana Villarreal, R. Gómez, M. Neumann-Spallart, N. Alonso-Vante and P. Salvador, *J. Phys. Chem. B*, 2004, **108**, (39), 15172

The Author

Kasem K. Kasem is a Professor of Chemistry at Indiana University Kokomo, USA. He is interested in developments in the field of applied electrochemistry, especially in physical and analytical applications of chemically-modified electrodes. He also has interests in semiconductor electrochemistry, the electrochemical behaviour of polymeric thin films, activation and metallisation of polymers and photoelectrochemical studies at inorganic/organic interfaces.

